

Functionalized Boron Nitride Nanotubes with a Stannic Oxide Coating: A Novel Chemical Route to Full Coverage

Wei-Qiang Han and Alex Zettl*

Department of Physics, University of California at Berkeley, and Materials Sciences Division, Lawrence Berkeley National Laboratory, Berkeley, California 94720

Received November 7, 2002; E-mail: azettl@socrates.berkeley.edu

Because of their low dimensionality and high surface area-to-volume ratio, nanotubes possess highly unusual physical properties. Often these properties can be dramatically influenced by the surface addition of selected atomic or molecular species. Such functionalization can lead to a significant enhancement of properties relevant to technological applications. Recently, it has been demonstrated that carbon nanotubes, and carbon nanotubes functionalized with ultrathin foreign species coatings, represent a new type of chemical sensor capable of detecting small concentrations of molecules under ambient conditions.¹

In contrast to carbon nanotubes, boron nitride (BN) nanotubes have a uniform electronic band gap independent of the diameter and chirality of the tube, and in their native state are essentially electrical insulating.² The intrinsic electronic properties of BN nanotubes might be advantageously exploited for various applications, including sensors. For example, the insulating BN nanotube could serve as an electrically insulating and inert, high surface area nanoscale scaffold or template onto which sensor materials are attached. Alternatively, foreign chemical species attached to the BN nanotube, either directly or via an intermediate active coating layer, could electronically dope the nanotube and thus directly influence its electrical conductance. Despite this obvious potential, to our knowledge no successful methods have been reported for coating and thus functionalizing BN nanotubes.

For this work we selected the semiconductor stannic oxide (SnO₂) to coat BN nanotubes, motivated by the fact that stannic oxide-based films have been widely used as conductive electrodes, transparent coatings, heterojunction solar cells, and chemical sensors. The deposition techniques used for SnO₂-based films include chemical vapor deposition, sol-gel, precipitation, laser pyrolysis, sputtering, and evaporation.³ Recently, the production of SnO₂ nanobelts (width ≈ 200 nm) sensitive to CO and NO has been reported.⁴

Here we demonstrate a novel, simple, and efficient room temperature chemical route to fully coat BN nanotubes with a thin, nominally uniform layer of SnO₂. High-resolution transmission electron microscopy (HRTEM) examination of the coating reveals interconnected SnO₂ nanoparticles of a size between 1 and 5 nm. Typically, the coatings have a total thickness on the order of the constituent nanoparticle size.

Bare (i.e., unfunctionalized) BN nanotubes were first synthesized through a carbon nanotube substitution reaction followed by an oxidation treatment.⁵ The outside diameter of the BN nanotubes is usually less than 8 nm. The nanotubes are formed either as isolated units or as tubes arranged in aligned bundles; no attempt was made to separate the different configurations. Into 50 mL of distilled H₂O was placed 1.2 g of tin (II) chloride (anhydrous, Alfa, 99%), followed by 0.8 mL of HCl (38%). After the addition of 15 mg of BN nanotubes, this solution was sonicated for 5 min and then stirred for 1 h at room temperature. The formation of SnO₂ is

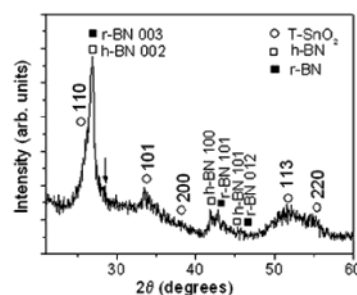


Figure 1. XRD spectrum of the product, which is identified as a mixture of tetragonal SnO₂, hexagonal BN (h-BN) and rhombohedral (r-BN).

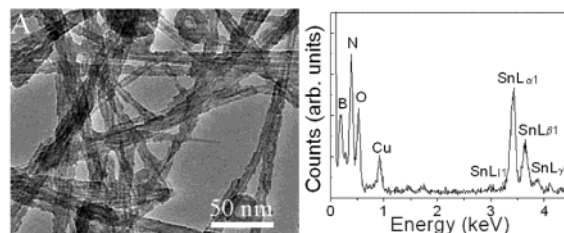


Figure 2. (A) Typical low-resolution TEM image of fully coated BN nanotubes. (B) Typical EDS spectrum of SnO₂-coated BN nanotubes. The atomic ratio of O and Sn is near 2.

represented as $2\text{SnCl}_2 + 2\text{H}_2\text{O} + \text{O}_2 \rightarrow 2\text{SnO}_2 + 4\text{HCl}$. The treated nanotube sample was then rinsed with distilled H₂O.

Products were characterized using the X-ray diffraction (XRD) of Cu K α radiation and HRTEM using a Philips CM200 FEG equipped with an energy-dispersive X-ray spectrometer (EDS).

Figure 1 shows results from an XRD measurement of the product. The diffraction peaks identify the sample as a mixture of tetragonal SnO₂ ($a = 4.755$, $c = 3.199$), hexagonal BN (h-BN), and rhombohedral BN (r-BN). The BN peaks are direct signatures of the BN nanotubes. BN nanotubes prepared by the carbon nanotube substitution reaction are typically composed of h-BN (two-layered repeated units) and r-BN (three-layered repeating units), in roughly equal volume fraction.⁵ The main peak of tetragonal SnO₂ (110) in Figure 1 almost overlaps with the main peaks of h-BN (002) and r-BN (003). The broad SnO₂ peaks indicate that the particle size is very fine. The small peak indicated by an arrow can be identified as orthorhombic SnO (112), demonstrating that a small amount of SnO also exists in the product.

For TEM analysis the material was first ultrasonically dispersed in ethanol and dropped onto a holey carbon-coated grid. Figure 2a is a typical low-resolution TEM image of the coated BN nanotubes. The BN nanotubes appear either as individuals or in bundles, and we observe that all nanotubes in the product have been fully coated with thin and uniform layers. The thickness of coating is usually less than 5 nm. Fullerene-like nanoparticles (FNPs) in the sample (a byproduct of the BN nanotube synthesis) have also been fully

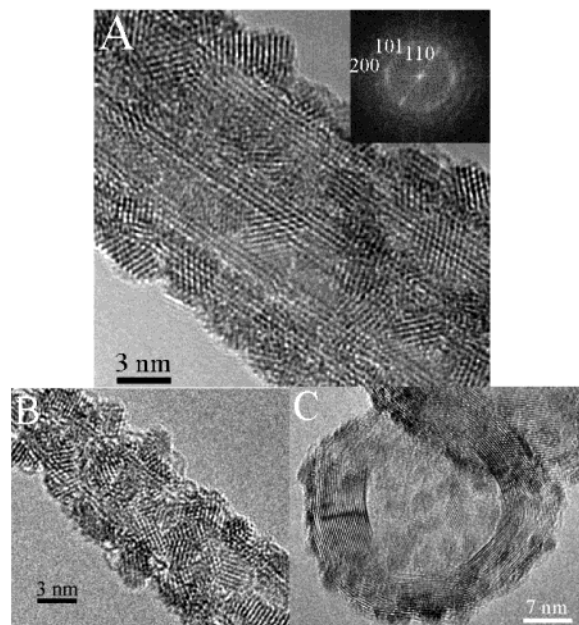


Figure 3. (A) HRTEM image of a BN nanotube bundle fully coated with SnO₂. (Inset) Corresponding FFT diffraction pattern. The three polycrystalline rings correspond to crystal faces of (110), (101), and (200) of tetragonal SnO₂. (B) HRTEM image of an individual double-walled BN nanotube fully coated with SnO₂. (C) HRTEM image of a SnO₂-coated BN fullerene-like nanoparticle.

coated. Chemical analysis using EDS indicates the presence of Sn, O, B, and N in the coated nanotubes and nanotube bundles (Figure 2b). The B and N signals originate from the supporting BN nanotubes. For the majority of the coated nanotubes and coated nanotube bundles, the atomic ratio of O to Sn is near 2. For a small number of tubes the coatings indicated O to Sn ratios between 1 and 2.

Figure 3 shows HRTEM images of coated BN nanotube bundles, coated individual BN nanotubes, and coated fullerene-like BN nanoparticles. Figure 3a shows a BN nanotube bundle fully coated with SnO₂. The coating is uniform, with an average thickness of about 3 nm. The coating layer is composed of nanocrystalline particles with sizes less than 5 nm. Fast Fourier transform (FFT) analysis of selected regions of the coating reveals details of the local SnO₂ structure. The inset to Figure 3a is the corresponding FFT diffraction pattern, which can be indexed to tetragonal SnO₂. The three polycrystalline rings correspond to crystal faces of (110), (101), and (200) of tetragonal SnO₂. Figure 3b is a HRTEM image of an individual double-walled BN nanotube fully coated with SnO₂. The coating is again uniform and thin, with average thickness of 3 nm. Here the coating layer is composed of nanocrystalline particles the sizes of which are less than 4 nm. Figure 3c is a HRTEM image of a fully coated fullerene-like BN nanoparticle. The SnO₂ coating layer follows the shape of the supporting nanoparticle template. Despite the simplicity of our preparation method, it is apparent that, independent of the precise morphology of the BN nanoparticles, surprisingly consistent and uniform nanometer-scale SnO₂ coverage is obtained.

It is useful to briefly contrast our coating method with other stannic oxide film preparation techniques. Aboaf et al. have deposited SnO₂ films by gas reaction of SnCl₄ with H₂O at 380–600 °C.⁶ Nagano prepared single-crystalline SnO₂ films by gas-phase reaction of SnCl₄ with O₂ at 900–1300 °C.⁷ Maudes et al., synthesized fine SnO₂ particle film by pyrolysis of SnCl₄·5H₂O and found particles of sizes 24–33 nm.⁸ All these results contrast with the present experiments, where SnCl₂ reacted with H₂O is used to synthesize uniform ultrafine (<5 nm) SnO₂ nanoparticle coatings under ambient conditions.

From a technological perspective, two extremes in the preparation of SnO₂-based sensors appear to be successful: thick films with nanocrystals of controlled size, and thin films with monolayers of nanocrystalline SnO₂.⁹ A SnO₂ thin film composed of nanocrystalline particles has shown high gas sensitivity and improved gas selectivity in comparison to sensors consisting of micrometer-sized grains.¹⁰ We anticipate that the SnO₂ thin coating with ultrafine SnO₂ nanoparticles produced in the present work will exhibit interesting physical properties relevant to technological applications. We also note our coating method is not restricted only to BN nanotubes and nanoparticles. We have used the identical method to fully coat both single- and multiwalled carbon nanotubes and carbon fullerene nanoparticles with SnO₂, and we believe that this method can be generally used to coat other structures with SnO₂. In addition, it may be possible to coat nanotubes with other substances by selecting different chlorides for this reaction.

In summary, a simple and efficient chemical reaction route was developed to synthesize SnO₂ coatings at room temperature. The resulting SnO₂ coatings on BN nanotubes and FNPs are thin and uniform, with uninterrupted coverage.

Acknowledgment. This research was supported in part by the Director, Office of Energy Research, Office of Basic Energy Sciences, Materials Sciences Division of the U.S. Department of Energy, under Contract number DE-AC03-76SF00098, administered through the sp² and Interfacing Nanostructures Initiatives.

References

- (1) (a) Collins, P.; Bradley, K.; Ishigami, M.; Zettl, A. *Science* **2000**, *287*, 1801. (b) Kong, J.; Franklin, N.; Zhou, C.; Chapline, M.; Peng, S.; Cho, K.; Dai, H. *Science* **2000**, *287*, 622. (c) Kong, J.; Chapline, M.; Dai, H. *Adv. Mater.* **2001**, *13*, 1384.
- (2) Chopra, N. G.; Luyken, R. J.; Cherrey, K.; Crespi, V. H.; Cohen, M. L.; Louie, S. G.; Zettl, A. *Science* **1995**, *269*, 966.
- (3) (a) Kohl, D. *J. Phys. D.* **2001**, *34*, R125. (b) Kruis, F.; Fissan, H.; Peled, A. *J. Aerosol Sci.* **1998**, *29*, 511.
- (4) Comini, E.; Faglia, G.; Sberveglieri, G.; Pan, Z.; Wang, Z. *Appl. Phys. Lett.* **2002**, *81*, 1869.
- (5) (a) Han, W.; Bando, Y.; Kurashima, K.; Sato, T. *Appl. Phys. Lett.* **1998**, *73*, 3085. (b) Han, W.; Mickelson, W.; Cumings, J.; Zettl, A. *Appl. Phys. Lett.* **2002**, *81*, 1110.
- (6) Aboaf, A.; Marcotte, V.; Chou, N. *Electrochem. Soc.* **1973**, *120*, 701.
- (7) Nagano, M. *J. Cryst. Growth* **1984**, *67*, 639.
- (8) Maudes, J.; Rodriguez, T. *Thin Solid Film* **1980**, *69*, 183.
- (9) Barsan, N.; Schweizer-Berberich, M.; Gopel, W. *Fresenius' J. Anal. Chem.* **1999**, *365*, 287.
- (10) Ogawa, H.; Nishikawa, M.; Abe, A. *J. Appl. Phys.* **1982**, *53*, 4448.

JA0292501